

ESI

Optically monitoring the microenvironment of a hydrophobic cargo in amphiphilic nanogels: influence of network composition on loading and release

Clara López Iglesias^{1,2,†}, Ante Markovina^{1,†}, Nithiya Nirmalanathan-Budau³,
Ute Resch-Genger^{3,*}, Daniel Klinger^{1,*}

¹*Institute of Pharmacy, Freie Universität Berlin, Königin-Luise Straße 2–4, 14195 Berlin, Germany*

²*Department of Pharmacology, Pharmacy and Pharmaceutical Technology, I+D Farma group (GI-1645), Faculty of Pharmacy, Instituto de Materiales (iMATUS) and Health Research Institute of Santiago de Compostela (IDIS), Universidade de Santiago de Compostela, Campus Vida s/n, 15782 Santiago de Compostela, Spain*

³*Division Biophotonics, Bundesanstalt für Materialforschung und –prüfung (BAM), Richard-Willstätter Straße 11, 12489 Berlin, Germany*

E-Mail: daniel.klinger@fu-berlin.de; ute.resch@bam.de

[†] Equal contribution

Table of contents

Attenuated total reflectance – Fourier transform infrared spectroscopy (ATR-FTIR).....	2
Transmission electron microscopy (TEM).....	3
Dynamic light scattering (DLS)	4
Loading content of particle batches	5
Emission spectra (part A).....	6
Quantum yield of particles with different amphiphilicity (part A).....	7
Spectral deconvolution and % of second species (parts A and B)	8
Fluorescence data (part B)	9
Intensity-weighted lifetimes (part B).....	10
Maximum of emission and quantum yield of NR in DODA NGs during release.....	11

Attenuated total reflectance – Fourier transform infrared spectroscopy (ATR-FTIR)

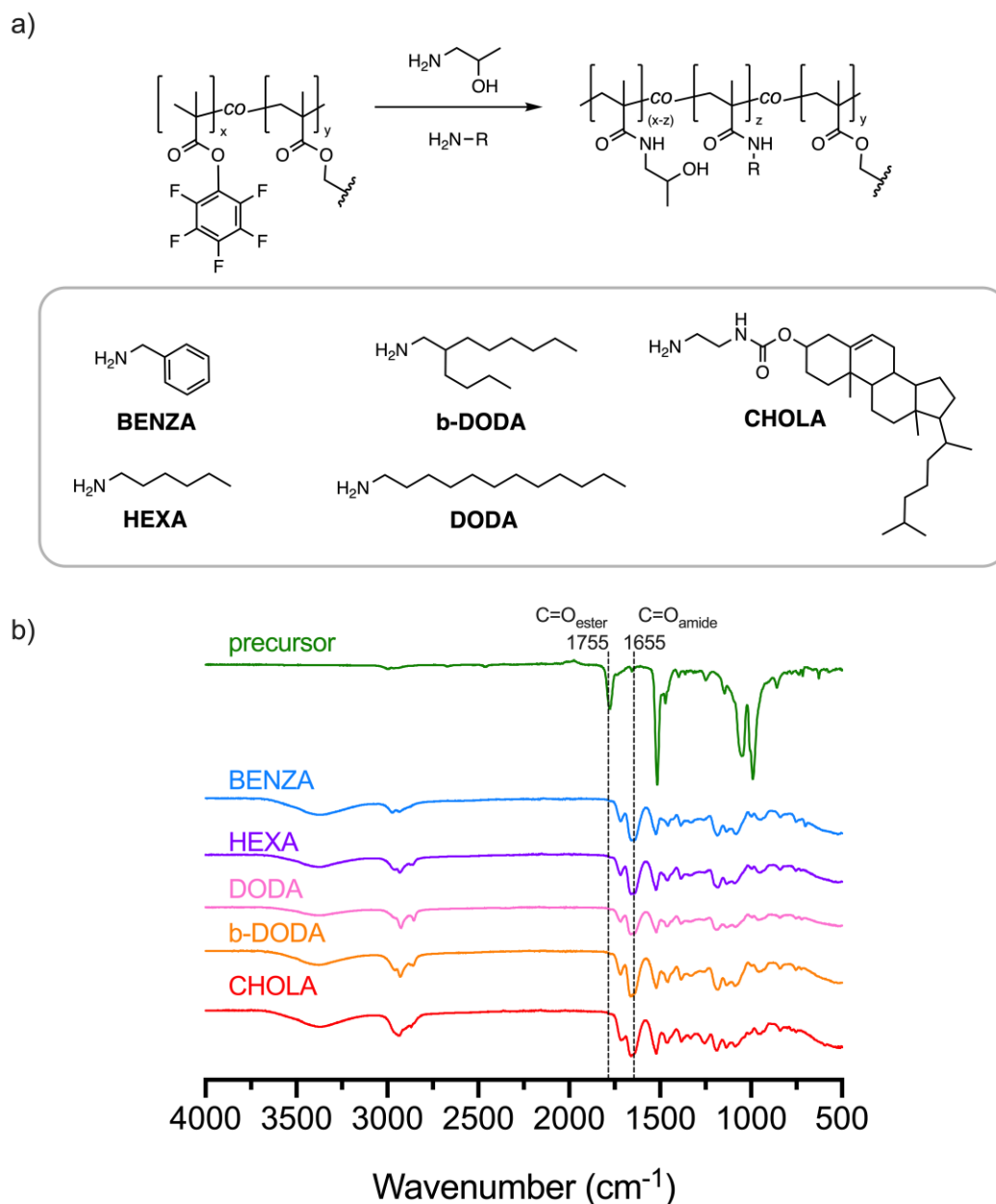


Fig. S1. Amphiphilic NGs were obtained by functionalization of reactive precursor particles. (a) General scheme of particle functionalization with structures of all hydrophobic amines used. (b) IR spectra of particles containing different hydrophobic groups. Disappearance of the peak at 1775 cm^{-1} (ester bond of the precursors) and apparition of a new peak at 1655 cm^{-1} (new amide bond) confirmed successful functionalization.

Transmission electron microscopy (TEM)

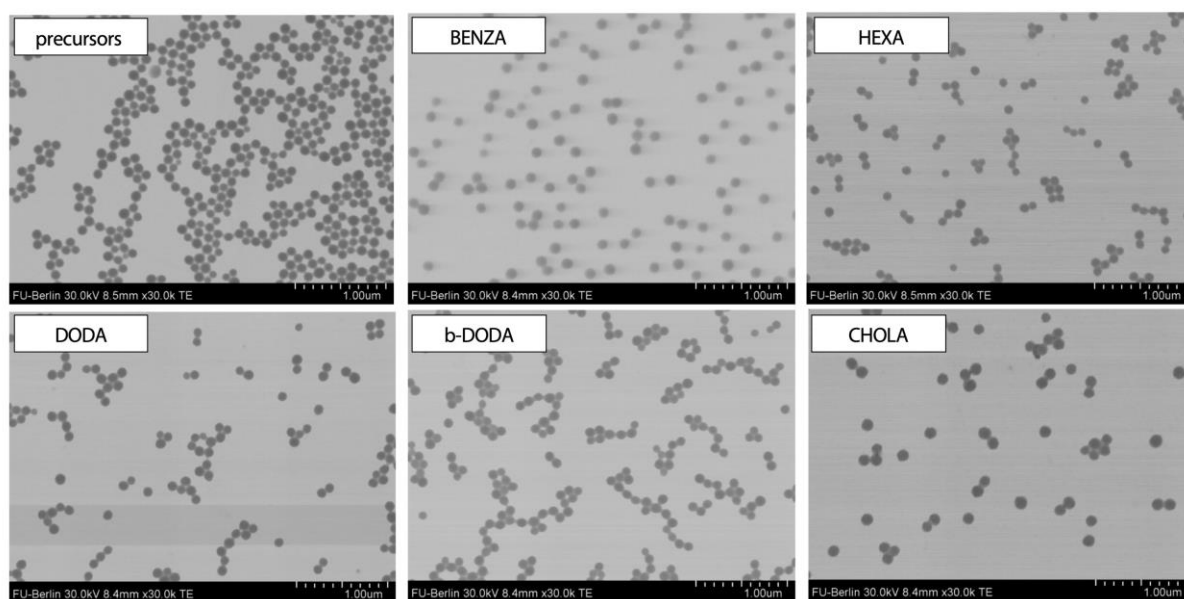


Fig. S2. TEM images of the particle precursors and particles functionalized with different hydrophobic groups. Functionalization did not have any influence on the appearance and homogeneity of the particles.

Dynamic light scattering (DLS)

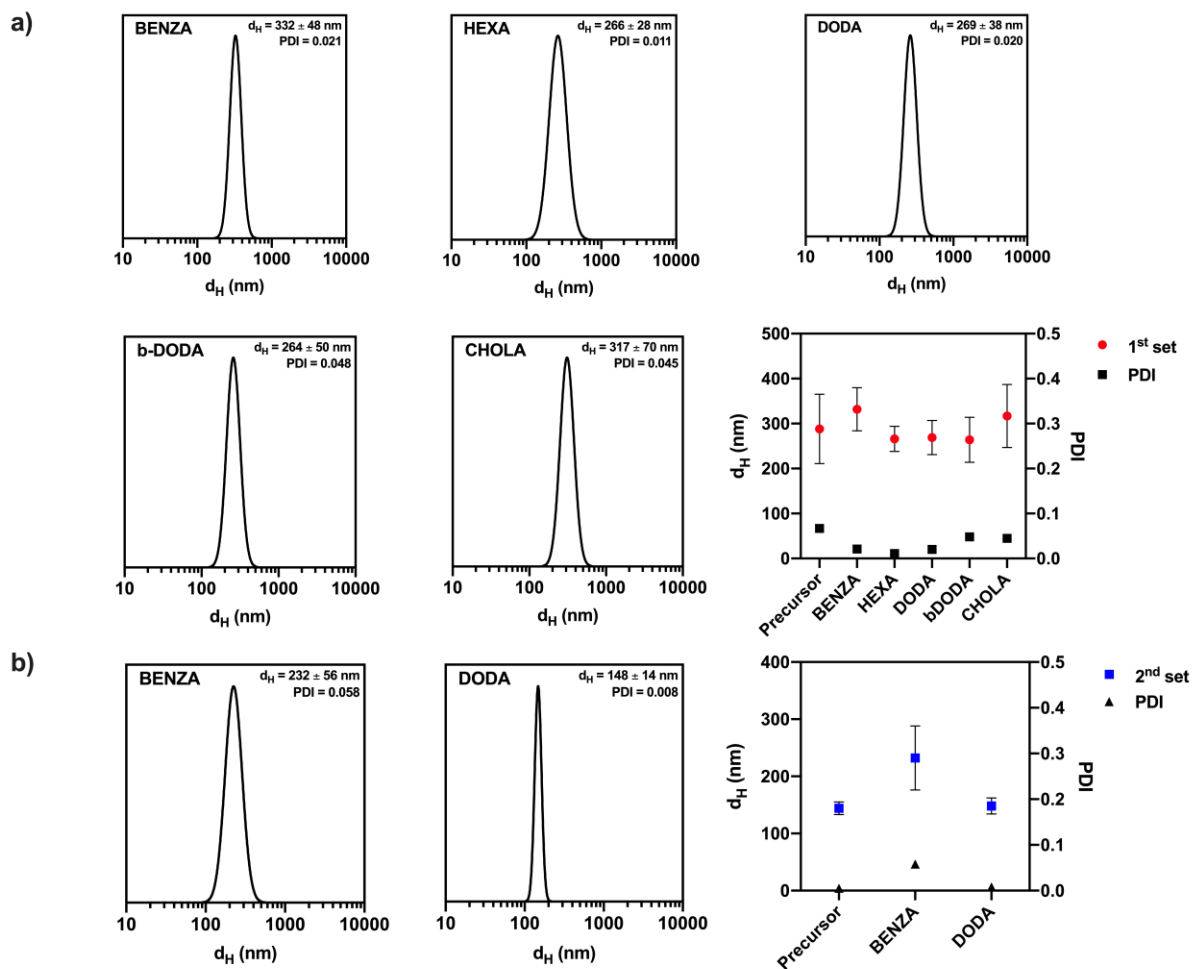


Fig. S3. DLS data of the first (a) and second (b) batches of particles. All particles were measured in water, except to the precursors which were swollen in DMF. In each set, the BENZA NGs show an increased particle size with respect to the rest of the NGs in the set. We suggest that this can be attributed to their more hydrophilic character and higher swelling degree in water.

Loading content of particle batches

The different nanogels were loaded using acetone as co-solvent, which was then evaporated causing the entrapment of NR inside the polymer network and precipitation of excess NR in water. After separating the excess dye by filtration, the NR-loaded particles were freeze-dried and resuspended in DMSO to photometrically determine the NR loading content and entrapment efficiency. For the NR feed ratios of 0.03 and 0.3 wt.%, quantitative loading is assumed since the feed ratios are below the previously determined maximum NR loading capacity of the ANGs and was also experimentally confirmed by us (see Fig. S4a). Only for BENZA-NR0.3 we observed a slight deviation from this trend, probably due to its more hydrophilic character. For high feed ratios like 3 and 10 wt.%, the encapsulation efficiency was reduced to actual LC values of 0.6 and about 1.5 wt.% (see Fig. S4b).

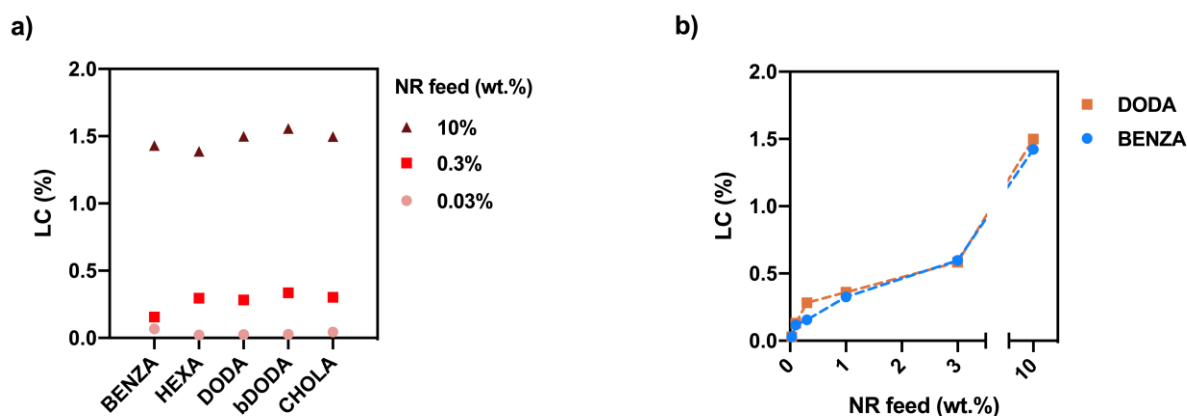


Fig. S4. Loading content of different NGs for the different NR feeds. (a) First batch with different types of NGs and (b) second batch with a larger set of NR concentrations. It is noteworthy that these ANGs are smaller than those in part A ($\Delta d_h = 100$ nm) (Fig. S3). However, the obtained LC is independent of particle size, i.e., it is similar for all particles of same composition and feed ratio. This suggests a similar spectroscopic behaviour.

Emission spectra (part A)

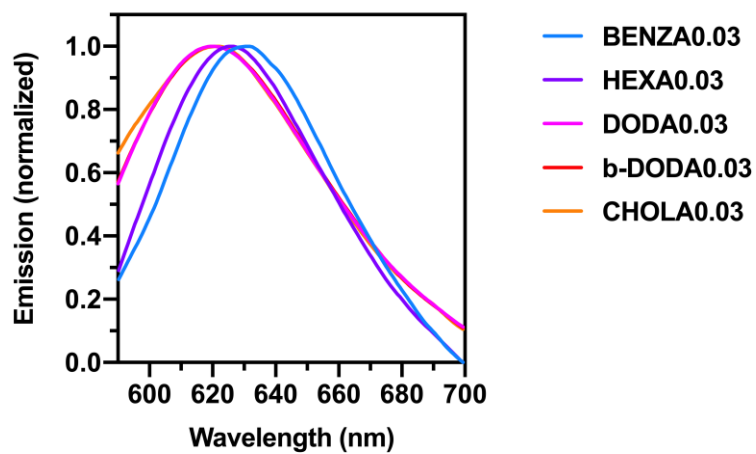


Fig. S5. Normalized emission spectra of NGs of different amphiphilicity loaded with NR at a feed ratio of 0.03 wt.%. Only slight differences in the maximum of emission were observed for BENZA and HEXA NGs.

Quantum yield of particles with different amphiphilicity (part A)

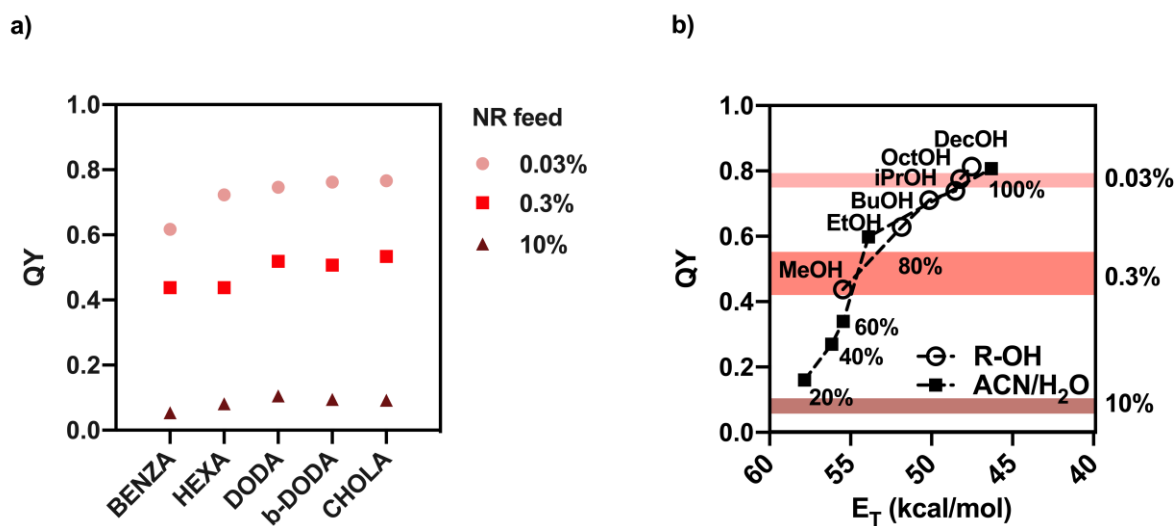


Fig. S6. Quantum yield (QY) of the particles of different amphiphilicity at three NR feed ratios (a) showed a strong dependence of NR feed on resulting QY, with noticeable differences between the different hydrophobic groups only at medium and low concentration. The values could be compared with QYs obtained for alcohols of different polarities and acetonitrile (ACN)/water mixtures of varied concentrations.

Spectral deconvolution and % of second species (parts A and B)

Table S1. Maximum wavelengths obtained in the spectral deconvolution and area % of each peak (area of the second emission band correlates with % of 2nd species).

Part	NG	NR feed (%)	First emission band		Second emission band		R ²	
			λ (nm)	Area (%)	λ (nm)	Area (%)		
A	BENZA	0.03	632	100	-	-	0.9955	
		0.3	625	21	642	79	0.9999	
		10	621	12	663	88	0.9996	
	HEXA	0.03	628	100	-	-	0.9920	
		0.3	629	45	661	55	0.9998	
		10	622	13	661	87	0.9988	
	DODA	0.03	623	100	-	-	0.9904	
		0.3	624	47	656	53	0.9999	
		10	612	20	658	80	0.9975	
	b-DODA	0.03	623	100	-	-	0.9920	
		0.3	624	48	659	52	0.9998	
		10	624	30	663	70	0.9948	
	CHOLA	0.03	620	100	-	-	0.9970	
		0.3	628	49	660	51	0.9999	
		10	624	30	663	70	0.9979	
	B	BENZA	0.03	632	89	681	11	0.9993
			0.1	631	43	658	56	0.9999
			0.3	630	29	650	71	0.9998
1			628	34	653	66	0.9996	
3			629	5	642	95	0.9990	
10			632	19	653	81	0.9989	
0.03			618	100	-	0	0.9924	
DODA		0.1	614	47	646	53	0.9998	
		0.3	623	47	657	53	0.9995	
		1	620	37	650	63	0.9995	
		3	618	16	646	84	0.9990	
		10	612	13	655	77	0.9997	

Fluorescence data (part B)

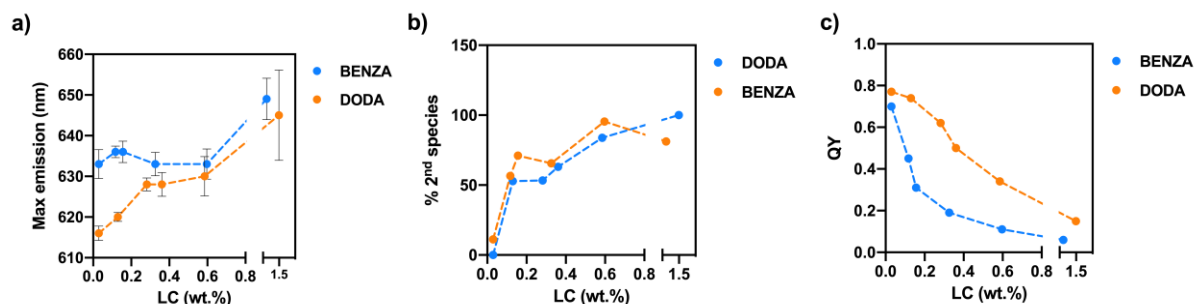


Figure S7. Emission spectra (a), percentage of second species (b), and quantum yield (c) of DODA and BENZA NGs at increasing NR contents. In general, emission maxima increased and quantum yield decreased with concentration.

In all samples, the previously determined trend of increasing emission maximum with LC is still visible over the broader NR LC range (ESI, Fig. S7a). Similarly, the QY decreases with LC in both ANG types (ESI, Fig. S7c). Comparing the BENZA to the DODA samples, it becomes obvious that $\lambda_{em,max}$ is always higher in BENZA than DODA, and QY is always lower. This supports the previously determined trend of an increasing contribution of second NR species in the more hydrophilic BENZA networks (ESI, Fig. S7b).

BENZA samples were red-shifted and had a lower quantum yield in comparison to DODA samples, suggesting a more hydrophilic nature. In the emission maxima, this difference is more pronounced at very low NR contents (LC < 40%). We suggest that as such low LCs NR is mostly molecularly dispersed in the hydrophobic domains where the emission spectra are governed by the interaction between NR and the hydrophobic domains (case A). Upon increasing the LC, this difference vanishes because NR is pushed to more hydrophilic environments or aggregates (cases B-C). This assumption is supported by the relative percentage of the second species (b). Here, it can be seen that for LC > 40 wt.% the second species dominates (> 50%), which suggests a more hydrophilic environment/aggregation.

Intensity-weighted lifetimes (part B)

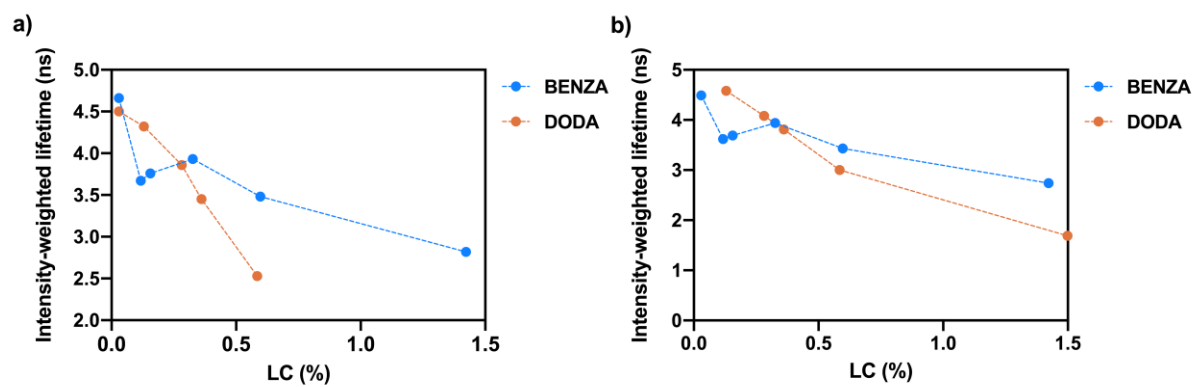


Fig. S8. Intensity-weighted lifetime of the first (a) and second (b) emission bands. BENZA NGs showed a sudden decrease in the lifetime intensity already at low concentrations.

Emission of NR in DODA NGs during release

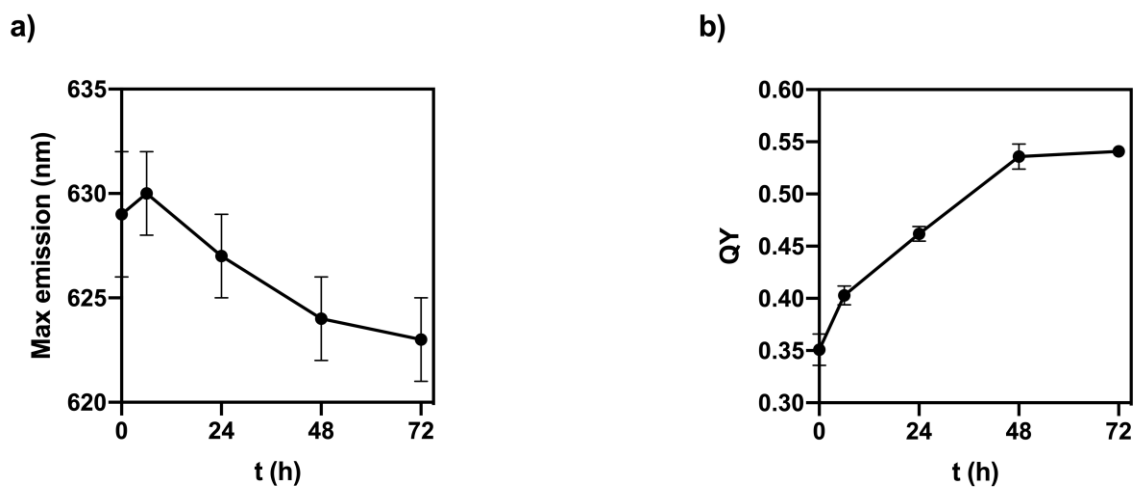


Fig. S9. Maximum of emission (a) and quantum yield (b) of remaining NR in DODA NGs at different time periods of release in water (37 °C). Decrease in the wavelength of maximum emission and increase in quantum yield indicated lower polarity of the microenvironment upon release.